IOPscience iopscience.iop.org

Home Search Collections Journals About Contact us My IOPscience

Surface reconstruction and many-atom models

This article has been downloaded from IOPscience. Please scroll down to see the full text article.

1991 J. Phys.: Condens. Matter 3 2755

(http://iopscience.iop.org/0953-8984/3/16/015)

View the table of contents for this issue, or go to the journal homepage for more

Download details:
IP Address: 171.66.16.96
The article was downloaded on 10/05/2010 at 23:08

Please note that terms and conditions apply.

J. Phys.: Condens. Matter 3 (1991) 2755–2767. Printed in the UK

Surface reconstruction and many-atom models

H Häkkinen, J Merikoski and M Manninen
Department of Physics, University of Jyväskylä, SF-40351 Jyväskylä, Finland

Received 9 October 1990

Abstract. The (110)(1 × 2) missing-row reconstruction of the seven FCC metals Ni, Pd, Pt, Cu, Ag, Au and Al has been studied using the effective medium theory (EMT). A clear trend in the tendency to reconstruct has been observed when going from the 3d metals Ni and Cu to 5d metals Pt and Au. The results are discussed together with some previous calculations using other many-atom models for total energy calculation in metals. The tendency to undergo reconstruction is found to be related to the anisotropy of surface energies on (111) and (110) surfaces. By investigating the effective two-body and three-body interactions on the surface it is shown that the missing-row reconstruction is related to the effective repulsion between adjacent nearest neighbour rows on the unreconstructed (110) surface. Restriction of the atomic interactions to the nearest neighbours only makes all the recent many-atom models favour the missing-row structure.

1. Introduction

It is a well-known fact that the first few layers of a clean metal surface exhibit relaxation in the vertical direction to optimize the electron density profile on the surface. The relaxation of the surface layers is sometimes connected with structural changes also in the horizontal direction, which is called reconstruction. One of the most commonly studied reconstruction patterns is the (1×2) missing-row reconstruction of the FCC(110) surface, which has been observed experimentally on Ir(110), Pt(110) and Au(110) [1–4]. It has been found to be involved with complicated multilayer relaxations, which provide a sensitive test for any approximate [5–9] or *ab initio* [10] method of total energy calculation in metals. However, a most important aspect is answering the question of why some FCC(110) metal surfaces do reconstruct, while some others (such as in Rh, Ni, Pd, Cu and Ag) do not. It is only recently that theoretical work has been directed in this way. Foiles [6] applied the semiempirical embedded atom method (EAM) [11] for Ni, Pd, Pt, Cu, Ag and Au and proposed the reconstruction to be connected with a large Cauchy discrepancy $C_{12} - C_{44}$. That would explain the missing-row structure of Pt and Au. He also derived effective pair and three-body interactions on the surface that explained qualitatively the reason for the reconstruction. Jacobsen and Nørskov [12] used a semiempirical model derived from the effective medium theory (EMT) [13] and found an increasing tendency for missing-row structure when going from Cu to Au in the noble metals. In their model, the reconstruction energy was related to the ratio C_{44}/B (B is the bulk modulus). The most recent work (to our knowledge) is the tight binding [14] study of Guillopé and Legrand [7], which gave results very similar to those obtained with the EAM for Cu, Ag and Au.

However, they showed that neither of the proposed criteria ($C_{12} - C_{44}$ and C_{44}/B) can fully explain the behaviour of Ir, Pt and Au with respect to the neighbouring FCC metals in the periodic table. Guillopé and Legrand were also able to derive detailed atomic interactions on the surface. Using these interactions within a generalized 2D Ising model they predicted a transition from the (1×2) missing-row structure to (1×1) disordered structure on Au(110) at temperatures well below the melting point, in accordance with an EAM result [15]. This kind of transition has in fact been suggested by the experiments above $T_c = 660$ K [16].

In this paper we go further than Jacobsen and Nørskov in their pioneering work [12] by calculating systematically the (110)(1×2) missing-row reconstruction energy for Ni, Pd, Pt, Cu, Ag, Au and Al using the recent parametrization of EMT by Puska [17]. The purpose of the paper is threefold. Firstly, it is shown that EMT is a convenient tool for looking at trends in various physical properties of materials, including the surface reconstructions. We found a realistic trend towards undergoing reconstruction when going from 3d metals Ni and Cu to 5d metals Pt and Au. Secondly, we want to compare our results with previous calculations [6, 7, 12] to find out the basic reasons for reconstruction. A simple geometric argument is found to explain the observed trends. On the other hand, the tendency to reconstruct can be related to the effective interactions between adjacent nearest neighbour rows on the unreconstructed surface. Thirdly, we found that it is essential to extend atomic interactions at least to the next-nearest neighbours. Restriction to the nearest neighbours only makes all the recent many-atom models favour the (1 × 2) missing-row structure—a point which has not been clearly pointed out previously.

We continue by giving a summary of the energetics of the (1 × 2) missing-row reconstruction in section 2. The effective medium formalism is briefly discussed in section 3. Our results are discussed in section 4 together with the previous calculations. Section 5 contains our conclusions.

2. Energetics of reconstruction

A schematic picture of the (110)(1 × 2) missing-row reconstructed surface is shown in figure 1. In the following we consider the energy difference between the reconstructed and unreconstructed surface. We do not include relaxation effects. We denote by $E(N_1, N_2, ...)$ the energy of an atom, when it has N_1 nearest neighbours, N_2 next-nearest neighbours, etc., according to the range of the atomic interaction.

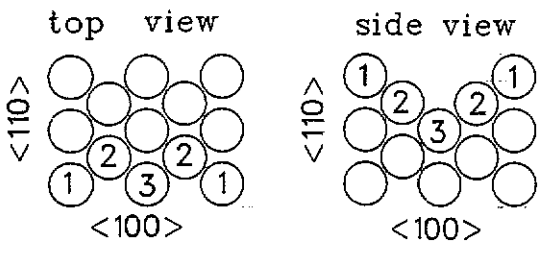

Figure 1. A schematic picture of the (110)(1 × 2) missing-row reconstructed surface. The numbers denote the atomic layers. Every second nearest neighbour row is missing, leading to the formation of (111) microfacets.

We first consider the nearest neighbour interactions only. The reconstruction energy $\Delta E^{(1\times 2)}$, defined as the energy difference between (1×2) missing-row structure and (1×1) unreconstructed structure per (1×1) unit cell, is [12]

$$\Delta E^{(1\times 2)} = \frac{1}{2}(-E(11) + 2E(9) - E(7)) \approx -2\frac{\mathrm{d}^2 E}{\mathrm{d}N_1^2}\bigg|_{N_1=9}. \tag{1}$$

If the next-nearest neighbours are also considered, the corresponding energy difference is

$$\Delta E^{(1\times 2)} = \tfrac{1}{2}(-E(11,4) + 2E(9,4) - E(7,4)) + \tfrac{1}{2}(E(7,2) - E(7,4)). \tag{2}$$

The first term in the right-hand side is again proportional to the discrete second derivative of $E(N_1, N_2)$ with respect to N_1 evaluated at the point $N_1 = 9$, $N_2 = 4$. The second term is clearly the formation energy of the step on the missing-row surface.

The (1×2) missing-row reconstruction can be thought to be a first step in a series where the surface exhibits (1×3), (1×4), etc., reconstructions which lead to larger (111) facets on the surface. The general form of the $(1\times n)$ reconstruction energy in the next-nearest neighbour model is

$$\begin{aligned}\Delta E^{(1\times n)} = {} & \left(\frac{n-1}{n}\right)(-E(11,4) + 2E(9,4) - E(7,4)) + \frac{1}{n}(E(7,2) - E(7,4)) \\ & + 2\left(\frac{n-2}{n}\right)(E(9,3) - E(9,4)).\end{aligned} \tag{3}$$

When the limiting case $(n \to \infty)$ is reached, the surface consists of two (111) facets whose summed area is larger than that of the original surface by a factor of $\sqrt{3/2}$. Equation (3) leads then simply to the difference in the surface energies $E_s^{(111)}$ and $E_s^{(110)}$

$$\begin{aligned}\Delta E^{(1\times\infty)} &= 2E(9,3) - (E(7,4) + E(11,4)) \\ &= \sqrt{3}E_s^{(111)} - \sqrt{2}E_s^{(110)}.\end{aligned} \tag{4}$$

A number of observations can be made from the equations above. Equation (1) clearly shows that *all* nearest neighbour models fail in describing the systematics of reconstruction. If one uses the nearest neighbour pair potential (which is, though, unreasonable in any case), $\Delta E^{(1\times 2)} \equiv 0$, because the energy function $E(N_1)$ is strictly linear. That is, a reconstructed surface makes no difference with respect to an unreconstructed surface. On the other hand, all the recent many-atom models [11, 13, 14, 18, 19] have a positive curvature in the energy function (determined by the positive curvature of the embedding function). *All* of them would therefore predict the (1×2) missing-row surface to be stable in any FCC metal. We can see from (2) that it is the inclusion of the next-nearest neighbours that makes the many-atom models realistic in describing reconstructions. The missing-row energy is now determined by the competition between the curvature of the energy function and the formation energy of the step on a (111) microfacet. That produces the differences between metals. It can be shown that the inclusion of the third-nearest neighbours does not change the qualitative picture of the energetics of reconstruction given by the next-nearest neighbours. Note that

in the pair potential models including the nearest and the next-nearest neighbours the sign of the step formation energy in (2) (and hence the reconstruction energy) is determined by the sign of the potential at the next-nearest neighbour distance (the positive sign leads to the reconstruction). Finally, by taking a derivative of $\Delta E^{(1\times n)}$ in (3) with respect to n one can see that it is a monotonic function and the minimum energy is obtained on the completely faceted surface. Therefore, possible minima in $\Delta E^{(1\times n)}$ for some $n < \infty$ are due to the relaxation effects [7].

3. Effective medium theory

The EMT has been described in detail by Jacobsen, Nørskov and Puska [13]. It gives a clear physical picture of the cohesion in metals and has been proved to be useful in various problems including those of describing surface structure [20, 21], impurities in metals [22], thermal bulk properties [23, 24] and large crystal defects such as dislocations [25].

The EMT is strongly based on the density functional theory [26]. Basic parameters are determined from the calculations for an atom in a homogeneous electron gas [27]. This fact has both positive and negative consequences for the use of the theory in real problems. Among the recent many-atom models, EMT is the one least based on empirical data. This implies a good transferability of the theory, which tempts one to use EMT in explaining the origin of the trends in various physical properties between materials. This is one of the motivations of the present work. On the other hand, one cannot always expect to get quantitatively good results when using EMT. The background model of the atom in a homogeneous electron gas makes EMT the model best suited for simple or sp-bonded metals [28]. For a proper treatment of transition metals, a one-electron energy correction (arising from the d–d interaction) should be included [13]. That has not been done in our systematic calculation, but we can qualitatively estimate the effect of the d–d interaction on our results for Ni, Pd and Pt, as shown in subsection 4.1.

It is not our intention to rewrite the detailed working formulas in EMT, discussed previously in numerous publications [13, 20, 22, 24, 25]. Here we only note that the total energy of a metallic system in EMT can be written in a form common to all recent many-atom models

$$E_{\mathrm{tot}} = \sum_{i=1}^{N}\left(F(\rho_i) + \frac{1}{2}\sum_{j\neq i} U(r_{ij})\right) \tag{5}$$

where F is a density-dependent many-atom energy function and $U(r)$ is a pair potential. ρ_i is a superposition of pair functions ('atomic densities')

$$\rho_i = \sum_{j\neq i} \rho^{\mathrm{a}}(r_{ij})\,. \tag{6}$$

The original EMT formalism was derived by supposing that only the nearest neighbours in the FCC lattice contribute to the background electron density of a certain atom. Because of the use of exponential functions in the pair potential U and in the density sum $\sum \rho^{\mathrm{a}}$ it is straightforward to extend the range of the atomic interactions in EMT.

This allows the inspection of the importance of these longer range interactions in various situations [24, 25].

In the present work we use EMT parameters published recently by Puska [17]. In addition we need one parameter (specifically η_1), which cannot accurately be calculated from first principles but is extracted for each metal from the experimental elastic constant C_{44} [29]. This is the only experimental input to our calculations. For a more detailed discussion of the EMT the reader is referred to [13, 30, 31].

4. Results and discussion

4.1. Reconstruction energies

To show qualitatively the influence of the inclusion of the next-nearest neighbours on the cohesive energy in EMT we show in figure 2 the energy functions $E(N_1)$ and $E(N_1, N_2)$ for copper in the range $6 \leq N_1 \leq 12$. It is seen that the cohesive energy is determined mainly by the nearest neighbours. Losing one next-nearest neighbour changes the energy of a copper atom by less than one per cent of the cohesive energy. However, as we concluded in section 2, the next-nearest neighbours are essential in determining the reconstruction energy. Note that the magnitude of the step formation energy (the second term in (2)) can be directly read from figure 2 ($\approx$ 60 meV/atom in Cu).

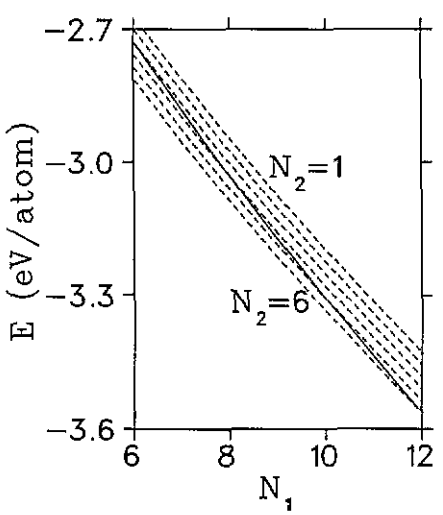

Figure 2. The energy of a copper atom as a function of the number of the nearest neighbours N_1 in EMT. The full curve is the result from the nearest neighbour formalism and the broken curves are the energies calculated from the extended EMT with the nearest and the next-nearest neighbours. The uppermost and the lowermost of the broken curves are $E(N_1, 1)$ and $E(N_1, 6)$, respectively. $E(12) = E(12, 6)$ by definition.

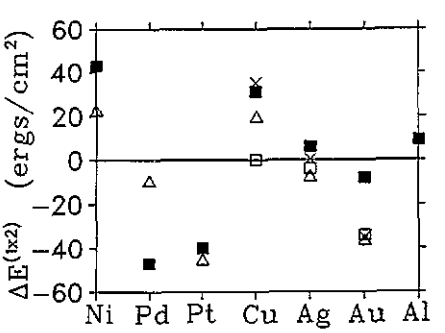

Figure 3. The reconstruction energies for Ni, Pd, Pt, Cu, Ag, Au and Al calculated from the recent many-atom models: EMT (this work, filled squares), EMT [12] (open squares), the EAM [6] (triangles) and the tight binding model [7] (crosses).

The unrelaxed reconstruction energies obtained in this work for Ni, Pd, Pt, Cu, Ag, Au and Al are shown in table 1 together with all the recent results from many-atom models of which we are aware. Table 1 contains also the *ab initio* results of Ho and Bohnen [10] for gold. A direct observation from table 1 is that the inclusion of relaxation does not change the trends among materials. Figure 3 shows the results obtained in this work together with the EAM results [6], the previous semiempirical EMT results of Jacobsen and Nørskov [12] and the tight binding results [7] to facilitate the comparison of systematics.

Table 1. The (110)(1 × 2) missing-row reconstruction energy for Ni, Pd, Pt, Cu, Ag, Au and Al calculated in this work compared with some recent results from other many-atom models: the embedded atom method (EAM) [6], the tight binding model (TB) [7] and the glue model for gold [8]. The last lines show the *ab initio* results of Ho and Bohnen (HB) for gold [10]. Also included are the results from the semiempirical EMT calculation of Jacobsen and Nørskov [12]. The asterisk denotes the metals that are experimentally known to exhibit the (110)(1 × 2) missing-row structure. The energies are in ergs cm^{-2}.

		Ni	Pd	Pt*	Cu	Ag	Au*	Al
EMT (*this work*)	unrel.	43	−47	−40	31	6	−8	9
EMT [12]	unrel.				0	−4	−34	
EAM [6]	unrel.	22	−10	−46	19	−8	−37	
	rel.	21	−6	−34	18	−6	−29	
TB [7]	unrel.				35	0.3	−35	
	rel.				33	0.7	−23	
Glue [8]	unrel.						−174	
	rel.						−242	
HB [10]	unrel.						−30	
	rel.						−70	

It is seen from table 1 and figure 3 that EMT, the EAM and the tight binding model all give the right trend towards undergoing reconstruction when one goes from Cu to Au in noble metals. The basic reason for the difference between the results of Jacobsen and Nørskov [12] and this work lies in the parametrization of the theory. In [12] the fall-off exponent of the induced electron density was approximated to be the same in Ag and Au as in Cu and the cohesive function was determined in a semiempirical way using experimental C_{44} and B.

The glue model [19] is an exception among all the recent many-atom models, because it is highly optimized for one particular element, namely gold. It predicts a strong tendency for Au to undergo the missing-row reconstruction, in accordance with experiments. However, since it is a nearest neighbour model, a similar parametrization would have made any FCC metal show missing-row reconstruction!

Previously, the transition metals Ni, Pd and Pt have been considered only by Foiles [6]. Figure 3 shows that both EAM and EMT are able to give a clear difference between Ni and Pt, in agreement with experiments. Quantitatively, EMT seems to fail in the case of Pd by predicting a clear tendency to undergo reconstruction, contrary to experimental results This failure can be understood in the following way. The parametrization of EMT from the jellium model leads to the overestimation of the bulk modulus by 80% and 90% for Ni and Pd, respectively. For other metals in this

work the corresponding values are +20% (Pt), +30% (Cu and Ag), −10% (Au) and +10% (Al). The crude overestimation of B in Ni and Pd is due to two main factors: an underestimation of the Wigner–Seitz radius and the omitting of the d–d interaction [13,22]. If we use the experimental lattice parameter and bulk modulus as input to the EMT parameters for the transition metals (as done in [22]), we find a more realistic trend in $\Delta E^{(1\times2)}$: 156, 50 and −20 ergs cm^{-2} for Ni, Pd and Pt, respectively. The more realistic trend for Ni, Pd and Pt in EAM results is then not a surprise, since the EAM contains the empirical values of the lattice constant, bulk modulus and elastic constants of each element.

EMT predicts the unreconstructed Al(110) to be stable, in agreement with experiments [32]. However, the energy difference between reconstructed and ideal surfaces is small. Recent experiments have shown that small amounts of impurity adsorbates (such as alkali metal atoms) may induce the (1×2) missing-row reconstruction on many FCC(110) surfaces [33]. The smallness of the energy difference for Al(110) could indicate that aluminium belongs to this category. Unfortunately, we are not aware of this kind of experiment having been performed on Al(110).

Finally, we want to point out that the jellium calculations behind the parametrization used in this work do not contain relativistic effects, which have been shown to be important in 5d metals [34]. This increases the inaccuracy of our results for Pt and Au. To summarize, the present theory cannot be used for the accurate quantitative comparison of the reconstruction energies in FCC metals but it is able to give realistic trends in the tendency to undergo reconstruction.

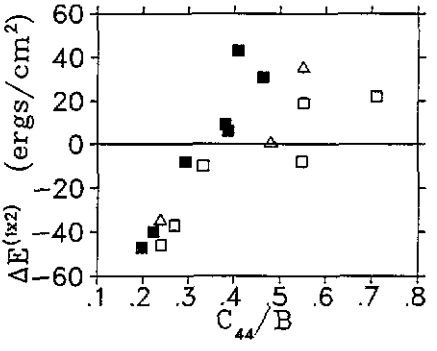

Figure 4. The reconstruction energy versus C_{44}/B in EMT (this work, full squares), in the EAM [6] (open squares) and in the tight binding model [7] (triangles).

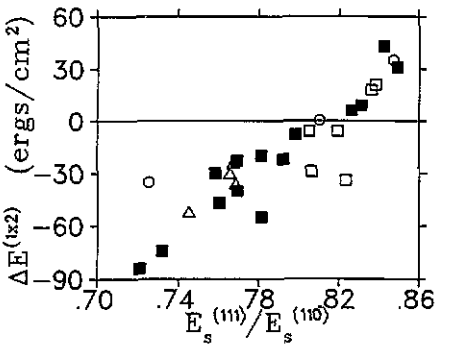

Figure 5. The reconstruction energy versus $E_s^{(111)}/E_s^{(110)}$ in EMT (this work, full squares), in the EAM [6] (open squares), in the tight binding model [7] (circles) and in the 'N-body potential' [35] (triangles).

4.2. Reconstruction versus elastic constants

More important than inspecting single reconstruction energies is the search for reasons underlying the observed trends. It is tempting to relate the tendency to undergo reconstruction to some measurable quantities of the bulk. As discussed in the Introduction,

the criteria suggested previously [6, 12] have been connected with the relations between the elastic constants. We have compared in figure 4 the calculated reconstruction energies from EMT (this work), the EAM [6] and the tight binding model [7] as a function of the calculated ratio C_{44}/B. Jacobsen and Nørskov [12] have shown that the reconstruction energy in EMT is approximately linear in C_{44}/B. Our results for all the seven metals confirm this suggestion. A similar correlation can be found also in other results shown in figure 4, although the 'critical ratio' seems to be model-dependent. Therefore, it is hard to find a 'universal' (model-independent) rule connecting the reconstruction and the elastic properties of all FCC metals. Moreover, as pointed out by Guillopé and Legrand [7], the elastic behaviour of Ir and Rh cannot be described by 'effective medium' or 'embedded atom' models without including some directionality in the atomic interactions.

4.3. Anisotropy of surface energies

The $(1 \times n)$ missing-row reconstruction leads to the formation of atomic-scale low-energy (111) facets. Therefore, it is reasonable to compare systematically the ratio of the calculated (111) surface energy to the (110) surface energy. We have collected in table 2 recent results for the (110), (100) and (111) surface energies calculated using EMT (this work), the EAM [11], 'the N-body potential' of Ackland *et al* [35], the tight binding model [7] and the glue model [8] together with the experimental estimate for each metal [36] (based on the surface tension of the liquid metal). Note that the EAM results contain the surface relaxation. A general conclusion from table 2 is that all many-atom models produce comparable surface energies on the low side of the experimental value. The only exceptions are the EMT value for nickel and the result from the glue model for gold.

Table 2 shows also the surface energy ratio $E_s^{(111)}/E_s^{(110)}$ calculated using the nearest neighbour EMT (when the missing-row structure is always favoured) and the model with the nearest and the next-nearest neighbours. The inclusion of the next-nearest neighbours seems to increase the surface energy ratio $E_s^{(111)}/E_s^{(110)}$. Figure 5 shows the calculated reconstruction energy as a function of the surface energy ratio. In our calculations, the critical ratio with respect to reconstruction is somewhere around 0.81. On the other hand, equation (4) gives the critical ratio for the $(1 \times \infty)$ reconstructed surface as $\sqrt{2/3} \approx 0.816$! In other words, the geometric criterion for the complete facetting seems also to be an essential factor behind the first step in the series leading to the facetting, namely the (1×2) missing-row reconstruction!

The applicability of this simple geometric argument can be readily tested using reported surface energies and reconstruction energies in other many-atom models, shown in table 2 and in figure 5. (The energy of the unrelaxed (111) surface for Cu, Ag and Au was not reported in [7] but we have calculated it using the given parametrization.) The model of Ackland *et al* is derived for Ni, Cu, Ag and Au and favours the reconstruction in all these metals [35]. As can be seen from table 2 and in figure 5, the corresponding surface energy ratio is below the geometric criterion value $\sqrt{2/3}$. A similar rule holds also for Cu, Ag and Au in the tight binding model (the ratio for Ag being just on the limit) and in the EAM as well as for Au in the glue model. The only exception is Pt in the EAM, where the ratio is just above $\sqrt{2/3}$ despite the clear tendency to undergo reconstruction. We have to note, however, that the EAM values contain the relaxation effects, which are likely to increase the calculated surface energy ratio. Unfortunately, we were not able to find the unrelaxed

Table 2. The surface energies of (110), (100) and (111) faces for the metals considered in this work. The first two columns are the results obtained in this work using the nearest neighbour (NN) EMT and the extended model with the nearest and the next-nearest neighbours (NNN). Also included are the results from the EAM [11], the 'N-body potential' by Ackland *et al* (ATVF) [35], the tight binding model (TB) [7] and the glue model for gold [8]. The last column shows the experimental surface energies estimated from the surface tension of the liquid metal [36]. The energies are in ergs cm^{-2}. The EAM results include surface relaxation. The numbers on the first row for each metal are the ratios of the surface energies on (111) and (110). Whenever the model predicts the (1×2) missing-row structure to be stable, the ratio is marked with an asterisk.

	EMT(NN)	EMT(NNN)	EAM	ATVF	TB	Glue	Experiment
Ni	0.781*	0.842	0.838	0.742*			
(110)	2530	2615	1730	1557			
(100)	2357	2349	1580	1449			2380
(111)	1976	2201	1450	1156			
Pd	0.721*	0.760*	0.819*				
(110)	1449	1473	1490				
(100)	1322	1313	1370				2000
(111)	1045	1120	1220				
Pt*	0.732*	0.769*	0.823*				
(110)	1428	1452	1750				
(100)	1308	1302	1650				2490
(111)	1045	1116	1440				
Cu	0.792*	0.849	0.836	0.765*	0.847		
(110)	1483	1532	1400	1250	1365		
(100)	1388	1385	1280	1147			1790
(111)	1175	1300	1170	956	1156		
Ag	0.781*	0.826	0.805*	0.757*	0.810		
(110)	908	931	770	830	790		
(100)	847	844	705	766			1240
(111)	709	769	620	628	640		
Au*	0.758*	0.798*	0.806*	0.741*	0.725*	0.699*	
(110)	844	862	980	872	650	2406	
(100)	781	778	918	796			1500
(111)	640	688	790	646	471	1682	
Al	0.769*	0.831					
(110)	797	823					
(100)	738	735					1180
(111)	613	684					

EAM surface energies for (110) and (111) in the literature.

As a conclusion, we find strong evidence that the simple geometric criterion for the complete facetting of (110) can alone determine the tendency to undergo (110)(1×2) missing-row reconstruction in all the recent many-atom models [37]. To our knowledge, this correlation (though intuitively clear) has not been previously theoretically shown to be so dominating. Bonzel *et al* [38] have given a similar conclusion based on the diffraction experiments on Pt(110) and Cu(110).

4.4. Effective interactions on the surface

In this subsection we will search the reason to undergo reconstruction by looking at the

effective interactions between atoms on the unreconstructed (110) surface. Foiles [6] has shown that by expanding the density dependent function $F(\rho)$ in (5) as a Taylor series around some average density ρ_0 it is possible to derive effective two-body, three-body, etc., interactions. Expanding $F(\rho)$ in (5) to second order gives

$$E_{\text{tot}} \approx \sum_{i=1}^{N}\left(F(\rho_0) + (\rho_i - \rho_0)F'(\rho_0) + \frac{1}{2}(\rho_i - \rho_0)^2 F''(\rho_0) + \sum_{j\neq i} U(r_{ij})\right)$$
$$= \sum_{i=1}^{N} E_0(\rho_0) + \frac{1}{2}\sum_{i=1}^{N}\sum_{j\neq i} V_{ij}(r_{ij}) + \frac{1}{6}\sum_{i=1}^{N}\sum_{j\neq i}\sum_{k\neq j\neq i\neq k} T_{ijk}(r_{ij}, r_{ik}) \qquad (7)$$

where

$$E_0(\rho_0) = F(\rho_0) - \rho_0 F'(\rho_0) + \tfrac{1}{2}\rho_0^2 F''(\rho_0)$$
$$V_{ij}(r_{ij}) = U(r_{ij}) + 2F'(\rho_0)\rho^{\text{a}}(r_{ij}) + F''(\rho_0)\rho^{\text{a}}(r_{ij})(\rho^{\text{a}}(r_{ij}) - 2\rho_0) \qquad (8)$$
$$T_{ijk}(r_{ij}, r_{ik}) = 3F''(\rho_0)\rho^{\text{a}}(r_{ij})\rho^{\text{a}}(r_{ik})$$

are the effective one-body, two-body and three-body potentials, respectively.

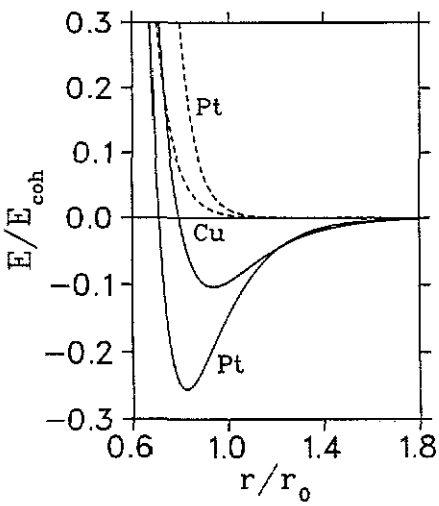

Figure 6. The effective pair potential $V(r)$ (full curves) and three-atom potential $T(r,r)$ (broken curves) calculated from EMT (interactions extended to the next-nearest neighbours) on Cu(110) and Pt(110). The energies are scaled with the cohesive energy E_{coh} and the distancies are scaled with the nearest neighbour distance r_0.

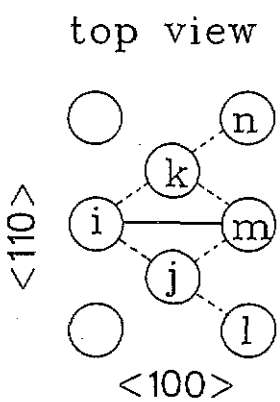

Figure 7. A schematic picture of the unreconstructed (110) surface (top view) showing how the atom i 'feels' the adjacent nearest neighbour row lmn. If the interactions are restricted to the nearest neighbours only, i interacts with l, m, and n only via the three-atom forces (broken lines) mediated by the second-layer atoms j and k. If the interactions are extended to the next-nearest neighbours there is also a direct pair force between i and m (full line).

We have plotted the effective two-body and three-body potentials (with $r_{ij} = r_{ik}$) derived from EMT for Cu and Pt in figure 6. The potentials have been evaluated using the nearest and the next-nearest neighbours and the value $\rho_0 \approx 0.58$ which is a typical EMT value for an atom on the unreconstructed (110) surface ($\rho_0 = 1$ in the bulk with the optimum density). The qualitative features of the potentials shown in figure 6 remain the same for all metals considered in this work: the three-body potential is purely repulsive and short ranged, whence the two-body part looks very much like a classical pair potential with a repulsive core and an attractive tail. With these interactions in hand, we can now determine the effective interaction between the nearest neighbour rows on the unreconstructed (110) surface. We do it by considering the change of the energy of atom i when an adjacent nearest neighbour chain is added on the surface (see figure 7). If the atomic interactions are restricted to the nearest neighbours, atom i 'feels' the neighbouring row lmn only with the three-atom interactions $T_{ijl}, T_{ijm}, T_{ikm}$ and T_{ikn} via the second-layer atoms j and k. This leads to an effective repulsion between adjacent nearest neighbour rows (the three-atom potentials derived from the nearest neighbour formalism are qualitatively similar to those shown in figure 6) and again explains why the missing-row structure is always favoured by the nearest neighbour model. The inclusion of the direct next-nearest neighbour pair interaction V_{im} makes the adjacent rows attract each other and then stabilizes the unreconstructed (1×1) surface in some metals. We have checked that the effective interactions between the first-layer atoms do really give the main contribution to the calculated energy differences between the reconstructed and unreconstructed surfaces for all the metals studied in this work. The effective surface atom interactions in EMT are then qualitatively similar to those given by the EAM [6], the tight binding model [7] and the field-ion microscope study of the (1×2) reconstructed Pt(110) [39].

5. Conclusions

We have studied the stability of the (110) surface in Ni, Pd, Pt, Cu, Ag, Au and Al using the effective medium theory (EMT). The only experimental input to our calculations is the elastic constant C_{44}, which was used in determining the value of one EMT parameter for each metal. All other parameters in the theory are based on the calculations of an atom in a homogeneous electron gas. This work shows that EMT is able to predict trends towards undergoing (1×2) missing-row reconstruction from 3d metals Ni and Cu to 5d metals Pt and Au. The only exception is Pd, which is predicted to favour the missing-row structure, contrary to experimental results. This behaviour can be related to the neglected d–d interaction in transition metals. The calculated reconstruction energies do not include relaxation effects. Previous works using other recent many-atom models have shown that the inclusion of relaxation does not change the observed trends in reconstruction energy.

The observed trends towards undergoing reconstruction can be explained in two independent ways. A simple geometric criterion $E_s^{(111)}/E_s^{(110)} < \sqrt{2/3} \approx 0.82$ is found to determine completely the tendency to reconstruct in our calculations. This criterion seems to explain also the results of other recent many-atom models and shows the dominant role of the anisotropy of surface energies underlying the reconstruction. Another way to understand the reconstruction is by examining the effective interactions between surface atoms. The tendency to reconstruct is shown to be connected

to the repulsion between the adjacent nearest neighbour rows on the unreconstructed surface.

For a realistic description of reconstruction energy it is essential to extend the atomic interactions at least to the next-nearest neighbours. Restriction to the nearest neighbours only makes all the recent many-atom models favour the missing-row structure.

Acknowledgments

The authors are grateful to M J Puska, J Timonen and S Valkealahti for useful discussions. This work has been partly supported by the Emil Aaltonen Foundation (HH) and by the Academy of Finland (JM).

References

[1] Moritz W and Wolf D 1985 *Surf. Sci.* **163** L655
[2] Chan C M and van Hove M A 1986 *Surf. Sci.* **171** 226
[3] Wrigley J D and Ehrlich G 1980 *Phys. Rev. Lett.* **44** 661
[4] Kellogg G L 1985 *Phys. Rev. Lett.* **55** 2168
[5] Daw M 1986 *Surf. Sci.* **166** L161
[6] Foiles S M 1987 *Surf. Sci.* **191** L779
[7] Guillopé M and Legrand B 1989 *Surf. Sci.* **215** 577
[8] Garofalo M, Tosatti E and Ercolessi F 1987 *Surf. Sci.* **188** 321
[9] Tománek D, Brocksch H J and Bennemann K H 1984 *Surf. Sci.* **138** L129
[10] Ho K M and Bohnen K P 1987 *Phys. Rev. Lett.* **59** 1833
[11] Foiles S M, Baskes M I and Daw M S 1986 *Phys. Rev.* B **33** 7983
[12] Jacobsen K W and Nørskov J K 1987 *The Structure of Surfaces II* ed J F van der Veen and M A van Hove (Berlin: Springer)
[13] Jacobsen K W, Nørskov J K and Puska M J 1987 *Phys. Rev.* B **35** 7423
[14] Rosato V, Guillopé M and Legrand B 1989 *Phil. Mag.* A **59** 321
[15] Daw M S and Foiles S M 1988 *Phys. Rev. Lett.* **59** 2756
[16] Kleban P, Hentschke R and Campuzano J C 1988 *Phys. Rev.* B **37** 5738
[17] Puska M J 1990 *Many-Atom Interactions in Solids* ed R M Nieminen, M J Puska and M J Manninen (Berlin: Springer)
[18] Finnis M W and Sinclair J E 1984 *Phil. Mag.* A **50** 45
[19] Ercolessi F, Bartolini A, Garofalo M, Parrinello M and Tosatti E 1987 *Phys. Scr.* T **19** 399
[20] Jacobsen K W and Nørskov J K 1988 *Phys. Rev. Lett.* **60** 2496
[21] Stoltze P, Nørskov J K and Landman U 1988 *Phys. Rev. Lett.* **61** 440
[22] Christensen O B, Stoltze P, Jacobsen K W and Nørskov J K 1990 *Phys. Rev.* B **41** 12413
[23] Stoltze P, Jacobsen K W and Nørskov J K 1987 *Phys. Rev.* B **36** 5035
[24] Häkkinen H and Manninen M 1989 *J. Phys.: Condens. Matter* **1** 9765
[25] Häkkinen H, Mäkinen S and Manninen M 1990 *Phys. Rev.* B **41** 12441
[26] Hohenberg H and Kohn W 1964 *Phys. Rev.* **136** B864
Kohn W and Sham L 1965 *Phys. Rev.* **140** A1133
[27] Puska M J, Nieminen R M and Manninen M 1981 *Phys. Rev.* B **24** 3037
[28] Quite recently, it has been shown that jellium calculations and EMT give a good description of the short range interactions between rare gas atoms (M J Puska and R M Nieminen 1991 *J. Phys.: Condens. Matter* **3** at press)
[29] Kittel C 1971 *Introduction to Solid State Physics* (New York: Wiley)
Simmons G and Wang H 1971 *Single Crystal Elastic Constants and Calculated Aggregate Properties: A Handbook* (Cambridge, MA: MIT Press)
[30] Jacobsen K W 1988 *Comment. Condens. Matter Phys.* **14** 129
[31] Jacobsen K W 1990 *Many-Atom Interactions in Solids* ed R M Nieminen, M J Puska and M J Manninen (Berlin: Springer)

[32] Jepsen D W, Marcus P M and Jona F 1972 *Phys. Rev.* B **6** 3684
Nielsen H B, Andersen J N, Petersen L and Adams D L 1982 *J. Phys. C: Solid State Phys.* **15** L1113
[33] Frenken J W M, Krans R L and van der Veen J F 1987 *Phys. Rev. Lett.* **59** 2307 and references therein
[34] Elsässer C, Takeuchi N, Ho K M, Chan C T, Braun P and Fähnle M 1990 *J. Phys.: Condens. Matter* **2** 4371
[35] Ackland G J, Tichy G, Vitek V and Finnis M W 1987 *Phil. Mag.* A **56** 735
[36] Tyson W R and Miller W A 1977 *Surf. Sci.* **62** 267
[37] The possibility of relating the tendency to undergo reconstruction to the anisotropy of surface energies was pointed out also by Jacobsen and Nørskov in [12].
[38] Bonzel H P, Freyer N and Preuss E 1986 *Phys. Rev. Lett.* **57** 1024
[39] Gao Q and Tsong T T 1986 *Phys. Rev. Lett.* **57** 452